East European Journal of Physics. **2.** 327-335 (2024)
DOI:10.26565/2312-4334-2024-2-38 ISSN 2312-4334

INFLUENCE OF GOLD ON STRUCTURAL DEFECTS OF SILICON

Sharifa B. Utamuradova[a], Shakhrukh Kh. Daliev[a], Alisher Khaitbaev[a], Jonibek J. Khamdamov[a]*, Ulugbek M. Yuldoshev[a], Anifa D. Paluanova[b]
[a]*Institute of Semiconductor Physics and Microelectronics at the National University of Uzbekistan, 20 Yangi Almazar st., Tashkent, 100057, Uzbekistan*
[b]*Nukus State Pedagogical Institute named after Ajiniyaz, Nukus, Uzbekistan*
**Corresponding Author e-mail: jonibek.uzmu@gmail.com*
Received April 8, 2024; revised April 28, 2024; accepted May 15, 2024

In this research, a comprehensive study of the effect of doping silicon with gold on the optical properties and morphology of silicon layers was carried out. For this purpose, the methods of Raman spectroscopy, Fourier transform infrared spectroscopy (FTIR), and scanning electron microscopy (SEM) were used. The results of the study showed that the transition from original silicon to gold-doped silicon leads to significant changes in the optical properties and morphology of the layers. Raman spectra showed characteristic peaks in the regions of 144, 304, 402, 464, 522, 948 and 973 cm^{-1}, associated with the violation of long-range order of the crystal lattice and the interaction of gold with silicon. The intensity and position of the peaks in the spectra allowed us to draw conclusions about structural changes, including a decrease in crystallinity and the formation of amorphous and nanocrystalline structures in the samples after treatment at 1373 K. New peaks in the Raman spectra associated with Au-Au stretching and the formation of new bonds Si-Au, confirm the processes in silicon layers when alloyed with gold. SEM studies provided information on the structure, chemical composition and arrangement of n-Si-Au and p-Si-Au samples. The spherical arrangement of gold atoms on the surface of single-crystalline silicon was experimentally established, which indicates the diffusion of gold and the formation of gold silicate, which introduces a positive charge to the interface. Morphological changes included an increase in the number of agglomerates with nanocrystals smaller than 7–9 nm and an increase in the transparency of the layer. These results indicate the possibility of improving the photosensitivity of heterostructures with a Si–Au composite layer due to the quantum-size and plasmonic effects of inclusions containing silicon and gold nanoparticles.
Keywords: *Silicon; Gold; Raman spectroscopy; Infrared spectroscopy; Diffusion; Scanning electron microscopy; Heat treatment; Temperature; Compound*
PACS: 33.20.Ea, 33.20.Fb

INTRODUCTION

In recent years, structured silicon has attracted significant interest, since silicon itself is a promising material not only for the field of electronics, but also for optoelectronics and solar cells [1-9]. Atoms of III-V elements (boron, arsenic, phosphorus and others) are widely used for doping silicon with fast-diffusing impurities, while gold is a typical slow-diffusing (deeply impurity) material. When an amphoteric gold atom diffuses into silicon via the Kick-out and Frank-Tranbull mechanisms, the ionized gold atom recombines with an n-type (or p-type) silicon electron (or hole). Diffusion gold atoms compensate for donors (or acceptors), which leads to an increase in silicon resistivity. Maximum resistance (Fig. 1.) can be achieved when the concentration of gold atoms compensates for the concentration of donors (or acceptors) [2].

Cold diffusion from the backside of the silicon device plays a crucial role in forming negative charge centers.

These centers compensate for the inherent positive surface charge at the silicon/silicon dioxide interface. Gold, interacting with silicon, forms an intermetallic compound characterized by the presence of an electrovalent bond (Fig. 2a.). This bond is less stable compared to the covalent bond between silicon atoms. Diffusion of gold from the front side of the silicon device leads to the formation of a gold silicate compound, introducing a positive charge at the interface [2-3]. One of the proposed models explaining the effects of gold centers at the silicon/silicon dioxide interface is based on a three-layer structure of the actual surface (Fig. 2b.). This model suggests the presence of different layers, including silicon, silicon dioxide, and a layer of gold silicate compound [3]. Interaction between these layers and the emerging charge centers plays a key role in the electrochemical and physical properties at the material interface.

The purpose of this work is to study the defect structure of silicon doped with gold, as well as the synthesis of composites on the Si-Au silicon surface by thermal firing at 1373 K. To study the structural and optical characteristics of the samples, methods of scanning electron microscopy (SEM image) and Raman spectroscopy (Raman spectrum) and Fourier transform infrared (FTIR) spectroscopy are used.

Raman spectroscopy is used to examine samples that are irradiated with monochromatic light, usually a laser. This technique allows the study of vibrational states that are the same as those observed in infrared spectroscopy (FTIR). Raman spectroscopy and infrared spectroscopy complement each other, since vibrations that are strong in the infrared spectrum are usually weak in the Raman spectrum, and vice versa. This allows for a more complete analysis of chemical

Cite as: Sh.B. Utamuradova, Sh.Kh. Daliev, A. Khaitbaev, J.J. Khamdamov, U.M. Yuldoshev, A.D. Paluanova, East Eur. J. Phys. 2, 327 (2024), https://doi.org/10.26565/2312-4334-2024-2-38

components and intramolecular interactions in samples. Raman spectroscopy is a non-destructive analysis method that allows you to study the physical properties of samples without changing their structure or composition. It also operates over a wide range from ultraviolet to near-infrared, making it a convenient and powerful tool for researchers.

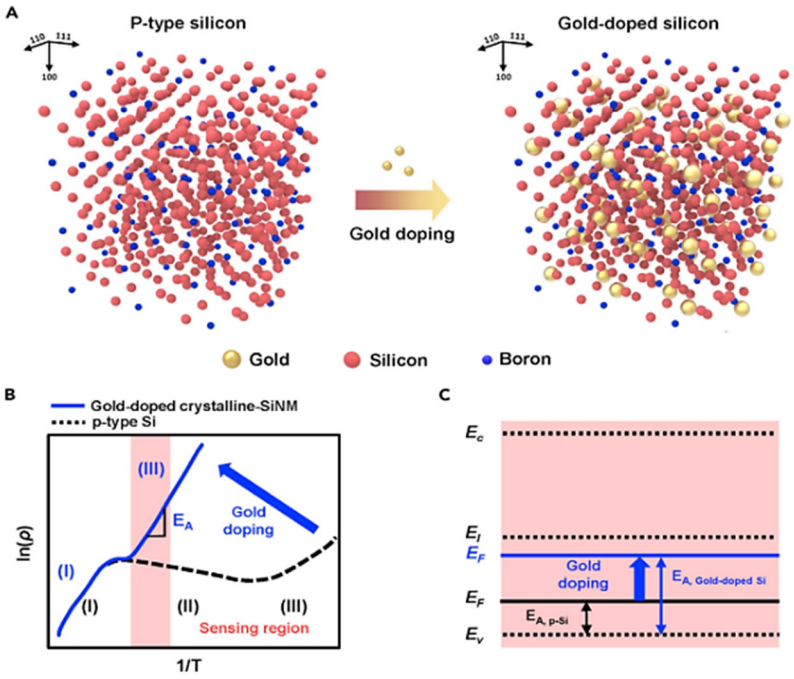

Figure 1. Changes in the properties of silicon after alloying with gold [2]
(A) Schematic illustration before and after doping silicon with gold; (B) Shift of resistivity curve after gold alloying process (I: inner region, II: outer region, III: freezing region); (C) Energy diagram of silicon after the gold doping process

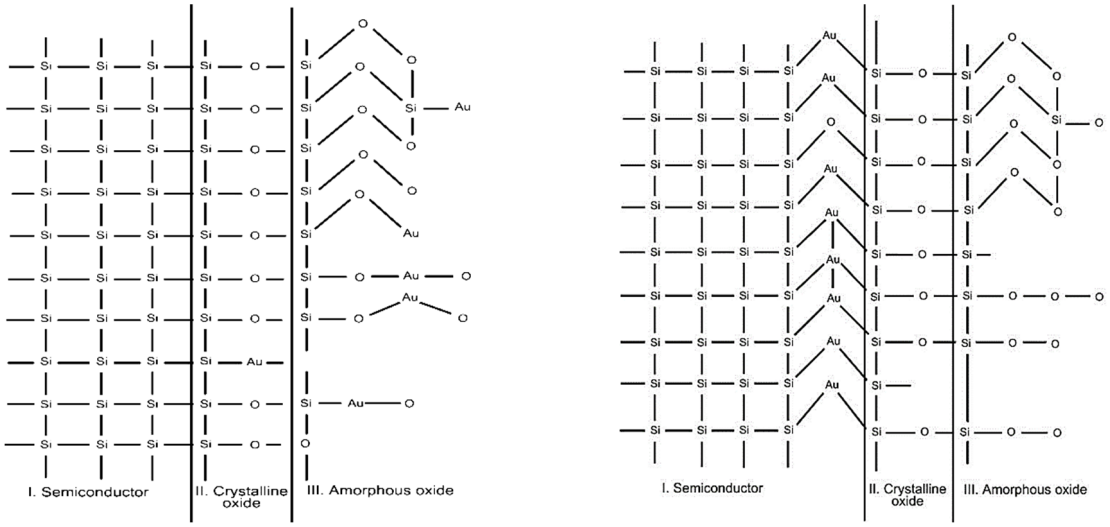

a) *Lattice structure of gold diffusion from the front of the silicon device.*

b) *Lattice structure of gold diffusion into silicon from the back of the substrate*

Figure 2. Lattice structure of gold diffusion into silicon [3]

MATERIALS AND METHODS

Studies using a ZEISS Gemini SEM 300 scanning electron microscope made it possible to obtain information about the structure, chemical composition and arrangement of n-Si-Au and p-Si-Au samples. The electron accelerating voltage was 20 kV, and the pressure in the sample chamber was 10^{-5} mmHg.

Raman spectra (Raman) and Fourier transform infrared spectroscopy (FTIR) were performed on six samples, including both types of pristine (n-Si and p-Si) doped with gold (n-Si<Au> и p-Si<Au>), as well as the resulting composites (n-Si-Au and p-Si-Au). The obtained spectroscopic data further confirmed the presence of amorphous and nanocrystalline structures on films annealed at 1373 K. Photoluminescence in the visible and near-infrared regions was observed in films containing both amorphous and crystalline particles.

To conduct the study, n-Si and p-Si silicon samples with an initial resistance of 0.3 Ohm·cm were selected. The process of doping with gold (Au) impurities was carried out sequentially using the thermal diffusion method. The samples were preliminarily chemically cleaned and etched with an HF solution to remove oxide layers from the surface. Then, films of high-purity gold were deposited onto a clean silicon surface by vacuum deposition in evacuated quartz ampoules at a vacuum level of $10^{-6}\div10^{-8}$ Torr using an oil-free vacuum pumping system.

Diffusion annealing of the samples was carried out at a temperature of 1373 K for 2 hours, followed by fast and slow cooling to uniformly dope the material and maximize the impurity concentration in silicon. Raman spectra were studied using a Confotec MR350 3D scanning laser Raman spectrometer using a 532 nm laser in the wavenumber range from 60 to 9500 cm^{-1}, as well as using a Bruker Senterra II Raman microscope using a 532 nm laser, in the wavenumber range from 50 to 4265 cm^{-1}, at room temperature. Infrared (IR) spectra were obtained using an FSM-2201 Fourier transform infrared spectrometer in the wavenumber range from 370 to 7800 cm^{-1} using FSpec software.

RESULTS AND DISCUSSION

Figure 3 shows an SEM image of gold-doped silicon. The spherical arrangement of gold atoms on the surface of monocrystalline p-type silicon doped with gold was experimentally established.

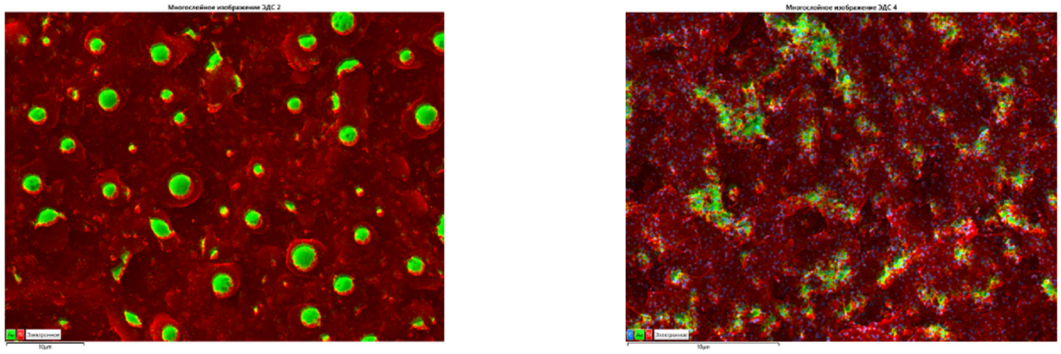

p-Si-Au n-Si-Au

SEM image of silicon doped with gold

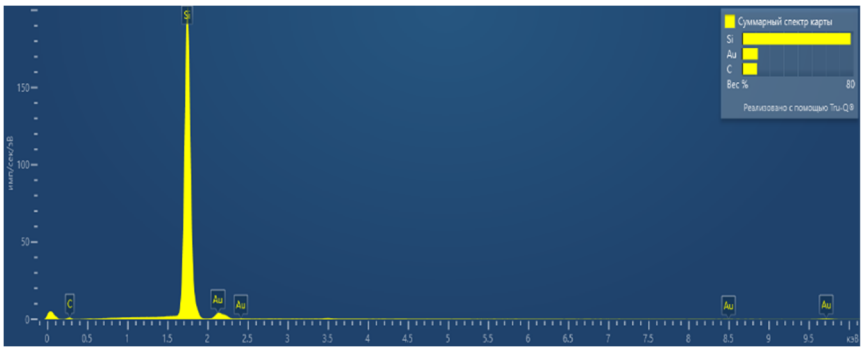

SEM spectrum of p-Si-Au

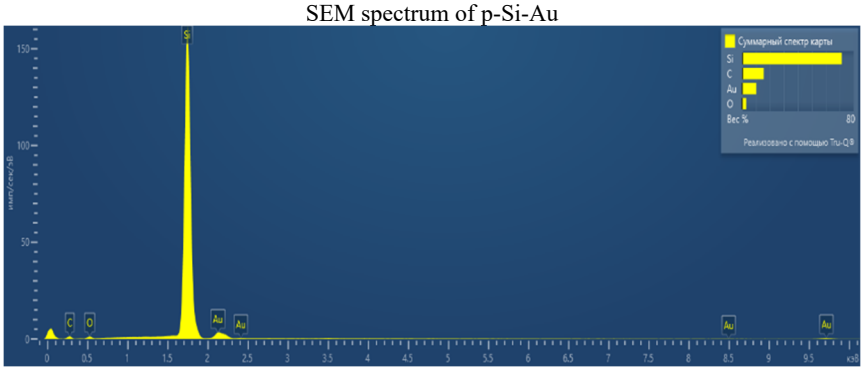

SEM spectrum of n-Si-Au

Figure 3. Surface properties of monocrystalline silicon doped with gold and subjected to heat treatment

Research results show that the structure of micro- and nanocomposites formed in silicon mainly depends on the diffusion time and cooling rate of the samples after diffusion annealing. The results of the study showed that thin films of gold with high silicon content were successfully prepared by thermal calcination, and n-Si-Au and p-Si-Au composites were prepared by thermal calcination at 1373 K. The obtained scanning electron microscopy data and Raman spectra were confirmed formation of both amorphous and nanocrystalline structures in films annealed at 1373 K.

Photoluminescence was observed and interpreted as interband recombination in nanoparticles larger than 2.5 nm, as well as carrier recombination through defect states in smaller nanoparticles.

Raman spectra for silicon samples doped with gold n-Si<Au> and p-Si<Au>, as well as composites obtained on their basis n-Si-Au and p-Si-Au, are presented in Figure 4.

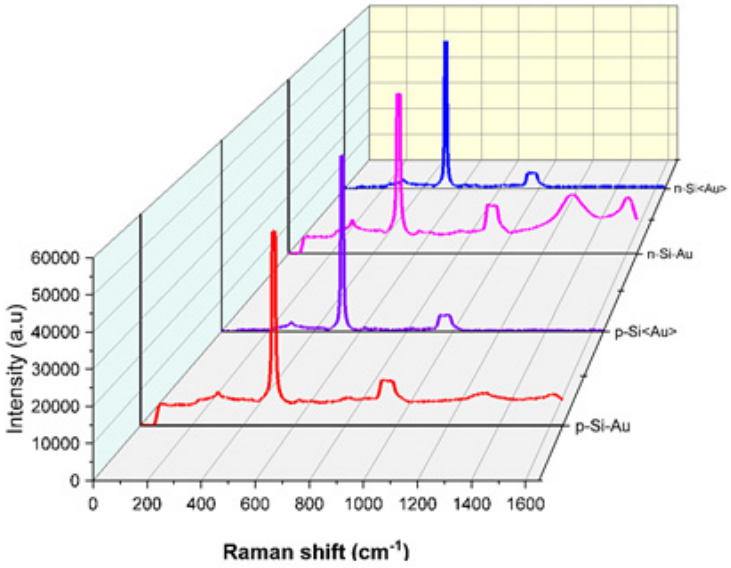

Figure 4. Raman spectrum of two types of gold-doped n-Si<Au> and p-Si<Au>, and n-Si-Au and p-Si-Au composites

The Raman spectrum of the sample (Fig. 4) includes bands with maxima in the regions of 144, 304, 402, 464, 522, 948 and 973 cm^{-1}. The appearance of such bands in Raman spectra is explained by the violation of long-range order (translation symmetry) of the crystal lattice, which removes the limitation imposed by the quasi-momentum conservation law (q=0). Therefore, in Raman spectra, phonons with all wave vectors q are allowed, which ultimately reproduce the density of vibrational states of the crystal lattice of the material under study [8-15].

The results show that the characteristic peaks of all four spectra examined are at the same spectral positions and the peak intensities are essentially identical. Similarly, to characterize the homogeneity of n-Si and the resulting n-Si-Au composites, we examined the most significant spectral regions (Fig. 5).

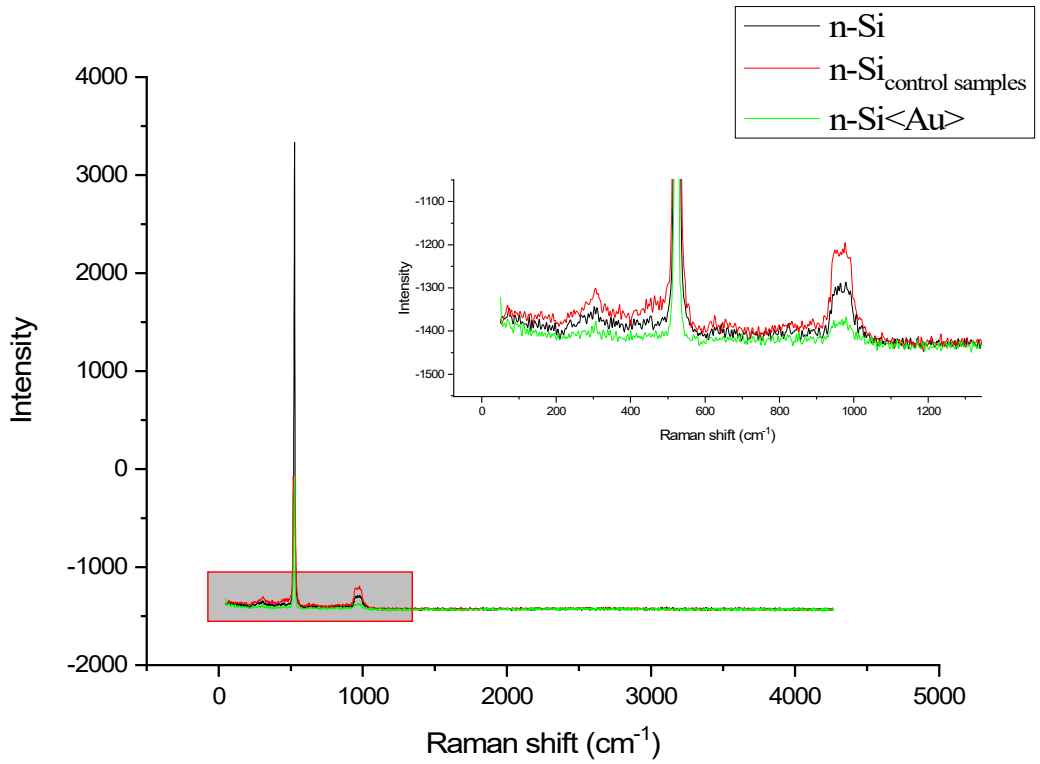

Figure 5. Comparative analysis of the Raman spectra of n-Si and gold-doped n-Si<Au>

Then we used the same method to analyze the Raman spectra of the most significant regions of the spectrum of p-Si and p-Si-Au composites obtained on their basis (Fig. 6). It was determined that in the studied spectra the main peaks appear at 566, 628, 674, 796, 948, 973, 1087, 1225, 1463, 1558, 1678, 1784, 2002, 2140 and 2325 cm^{-1}, which are consistent with literature data [11].

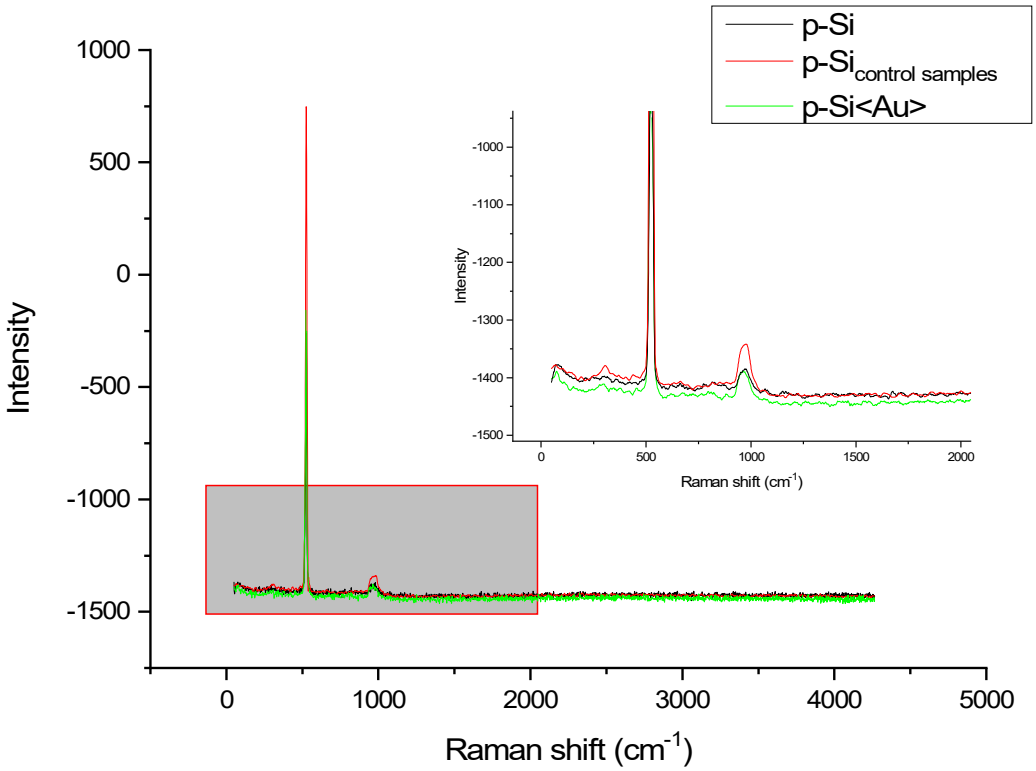

Figure 6. Comparative analysis of the Raman spectra of p-Si and gold-doped p-Si<Au>

From the data given in Fig. 5. and Fig.6. it is clear that, when moving from the original n-Si, p-Si to gold-doped n-Si<Au>, p-Si<Au>, the signals in the regions of 304 and 948 cm^{-1} undergo some changes, such as the intensity increases, they expand and will be mixed relative to the signals of the original n-Si, p-Si. It should be also pointed out that the main intense signal manifested in the region of 522 cm^{-1} upon transition from the original n-Si and p-Si to gold-doped n-Si<Au>, p-Si<Au> noticeably broadens. This, in turn, indicates a decrease in the crystallinity of the original n-Si and p-Si.

When studying the obtained spectra, accurate determination of the band of nanocrystals is extremely important, especially for films grown on n-Si and p-Si substrates. In nanocrystalline silicon films, the scattered light from the film is quite intense, but the scattering from the substrate is significantly reduced due to absorption in the film. This means that the shape and position of the band emanating from the nanocrystals should not be distorted when scattered on the substrate. However, in the resulting n-Si-Au, p-Si-Au composites, the filling factor is relatively small, which can be about 10%. The intensity of the scattered light from the Si nanocrystals is quite low, while the Raman line remains strong due to the n-Si substrate. From the given Fig. 5. and Fig.6, it can be seen that the strong band in all spectra has a maximum at 522 cm^{-1} and a width at half maximum of 4.3 cm^{-1}. It is necessary to take into account the fact that scattering from Si nanocrystals is quite weak and does not have a noticeable effect on the shape and position of the substrate strip. Since the exact intensity level of the scattered light from the n-Si and p-Si substrate cannot be determined, we conclude that it is impossible to correctly determine the size of Si nanocrystallites from the Raman spectra of the resulting low filling coefficient n-Si-Au, p-Si-Au composites.

Fourier transform infrared spectroscopy (FTIR) was used to further study the changes in gold-doped n-Si<Au> silicon from pristine n-Si. IR spectra in the region from 380 to 600 cm^{-1} were carefully studied to identify structural changes in n-Si and gold-doped silicon n-Si<Au>. The IR spectra of both the original n-Si and gold-doped silicon n-Si<Au> are presented in Figure 7a.

When analyzing using IR spectrometry both n-Si itself, as well as silicon doped with gold n-Si<Au>, in addition to the absorption of light by the atoms of the crystal lattice, there was also an absorption process associated with defects and present impurities. When studying the obtained IR spectra, the following patterns were revealed: absorption bands at 1107 and 513 cm^{-1} of crystalline silicon are associated with oxygen (one must take into account the fact that oxygen in crystalline silicon is located between the nodes and is an electrically neutral interstitial impurity) present in silicon, carbon in crystalline silicon exhibits one antisymmetry typical stretching (ν_{as}) vibration, the frequency of which is 609 cm^{-1}. n-Si doped with Au exhibits additional peaks in its IR spectra due to the presence of vacancies and defects in n-Si<Au>. The peaks at 513 cm^{-1} arise from the Si-Si stretching mode, and at 818 cm^{-1} from the wagging mode of hydrogen.

To consider changes in the IR spectra in the original n-Si and doped n-Si<Au> composition, we subsequently studied in detail the regions from 400 to 1650 cm^{-1} (Figure 7b). The resulting spectra clearly show all the changes that occur during the transition from n-Si to doped n-Si<Au>.

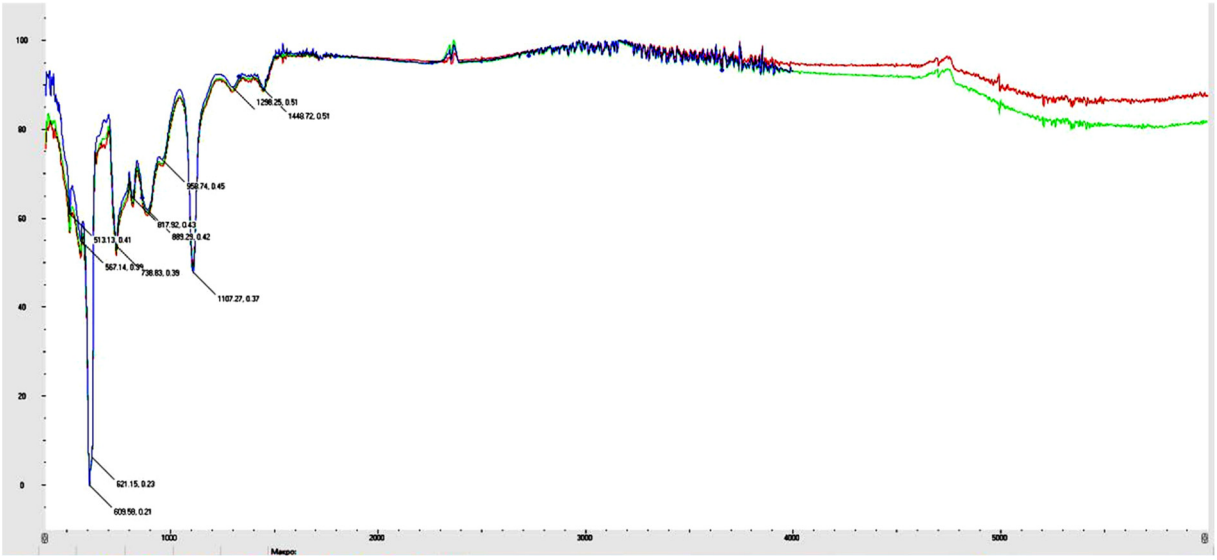

Figure 7a. IR spectrum of n-Si:
(red) n-Si; (green) n-Si$_{control}$; (blue) n-Si<Au>

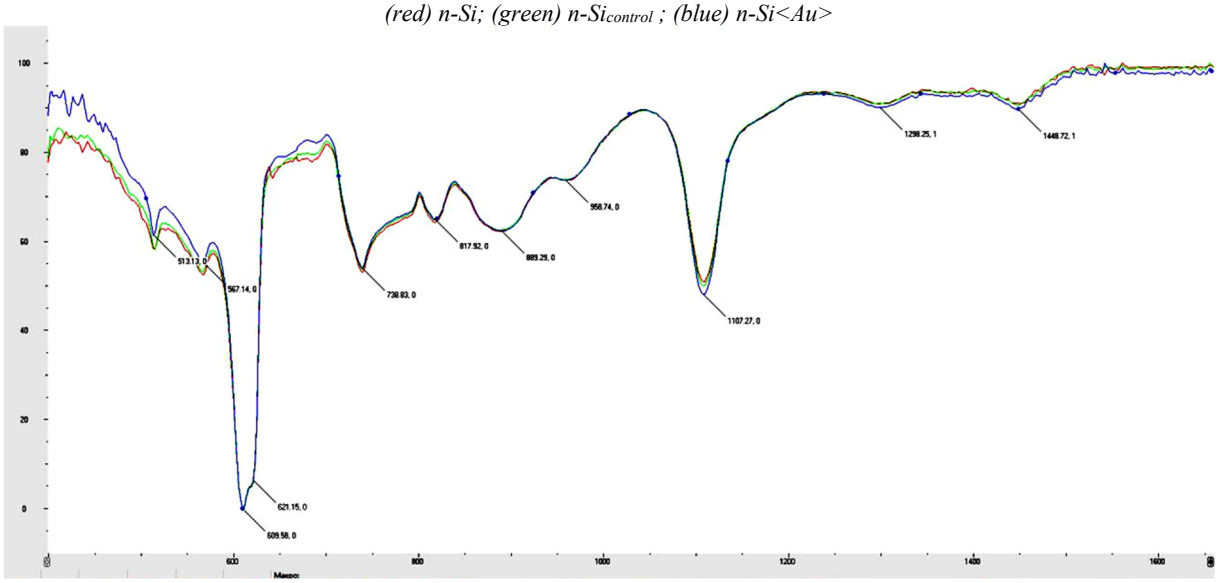

Figure 7b. IR spectrum of n-Si (region from 400 to 1650 cm^{-1}):
(red) n-Si; (green) n-Si$_{control}$; (blue) n-Si<Au>

A detailed study of the obtained IR spectra of n-Si, thermally treated n-Si and doped n-Si<Au> composition revealed the following patterns:

1) when moving from n-Si to thermally treated n-Si, some signals are relatively smoothed out (for example, the region from 400 to 500 cm^{-1}) and new signals appear, which can be explained by a mixing of characteristic frequencies;
2) upon transition from both types of n-Si (plain and control samples) to doped n-Si<Au> composition, for some characteristic frequencies (513, 609, 739 and 1107 cm^{-1}) the intensity noticeably increases and new signals associated with Au-Au stretching located between 2210 cm^{-1} and 2350 cm^{-1}. New signals at 2110 and 2124 cm^{-1} indicate the interaction of gold with silicon by the formation of new Si-Au bonds.

The same method was then used to analyze p-Si and doped p-Si<Au>. At the same time, it was determined that in the studied spectra the main peaks appear at 513, 609, 619, 739, 891, 1107, 1302, 1449 cm^{-1}, etc. The IR spectra of both the original p-Si and the doped p-Si<Au> are presented in Figure 8a.

To consider changes in the IR spectra in the original p-Si and doped p-Si<Au> composition, we subsequently studied in detail the regions from 400 to 1750 cm^{-1} (Fig. 8b). The resulting spectra clearly show all the changes that occur during the transition from p-Si to p-Si<Au> doping.

When comparing the obtained spectra of both types n-Si and p-Si, as well as n-Si<Au> and p-Si<Au> obtained on their basis, it should be noted that when going from n-Si<Au> to p-Si<Au> all peaks almost coincide but at the same time the intensity of the signals increases noticeably (comparison of Fig. 7b and Fig. 8b) [16-21].

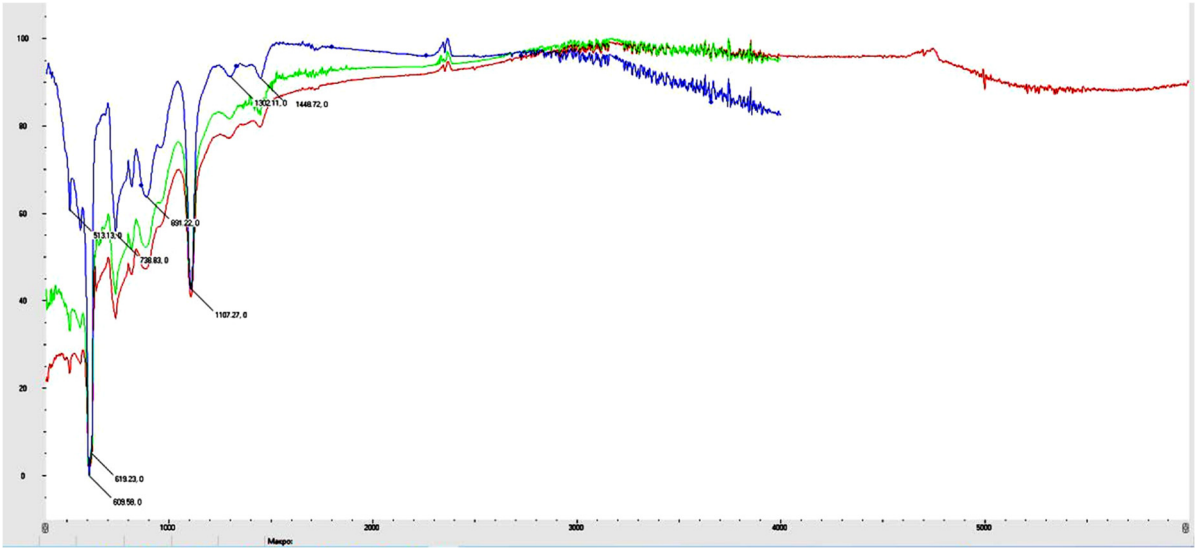

Figure 8a. IR spectrum of p-Si:
(red) p-Si; (green) p-Si$_{control}$; (blue) p-Si<Au>

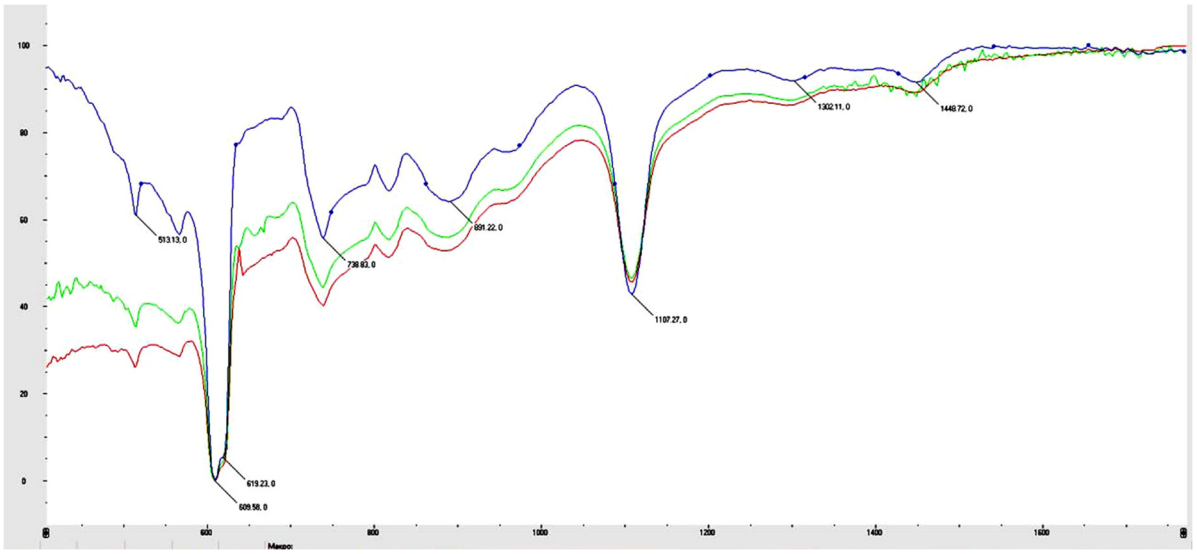

Figure 8b. IR spectrum of p-Si (region from 400 to 1750 cm^{-1}):
(red) p-Si; (green) p-Si$_{control}$; (blue) p-Si<Au>

CONCLUSIONS

The comprehensive analysis of silicon doped with gold and the subsequent synthesis of Si-Au composites have provided a wealth of insights into their structural and optical characteristics. Utilizing advanced analytical techniques such as scanning electron microscopy (SEM), Raman spectroscopy, and Fourier transform infrared spectroscopy (FTIR), we have uncovered significant transformations in the materials' properties. SEM imaging has offered a detailed view of the surface properties of monocrystalline silicon doped with gold, revealing a distinct spherical arrangement of gold atoms. This arrangement not only confirms successful doping but also hints at potential surface interactions and structural modifications induced by gold. Raman spectroscopy has been instrumental in identifying structural changes at the molecular level. The Raman spectra of gold-doped silicon samples and their resulting composites exhibited characteristic peaks indicative of altered vibrational states. Notably, the broadening and intensification of certain signals suggest the disruption of long-range order and the introduction of new vibrational modes due to gold doping. Further insights were gained through FTIR spectroscopy, which revealed shifts and enhancements in absorption bands associated with the interaction of gold with silicon. The emergence of new Si-Au bonds, as evidenced by specific peaks in the IR spectra, highlights the chemical modifications occurring upon gold doping.

The detailed analysis of these spectroscopic data underscores the intricate interplay between gold and silicon, leading to profound changes in the materials' structural, vibrational, and chemical properties. These findings are of significant importance for understanding the fundamental mechanisms underlying gold doping in silicon and have promising implications for the development of advanced optoelectronic devices and materials with tailored properties. In conclusion, this study contributes valuable insights into the complex behavior of gold-doped silicon and paves the way for future research aimed at harnessing these materials for a wide range of applications in electronics, photonics, and nanotechnology.

ORCID

Sharifa B. Utamuradova, https://orcid.org/0000-0002-1718-1122
Shakhrukh Kh. Daliev, https://orcid.org/0000-0001-7853-2777
Alisher Khaitbaev, https://orcid.org/0000-0001-9892-8189
Jonibek J. Khamdamov, https://orcid.org/0000-0003-2728-3832
Ulugbek M. Yuldoshev, https://orcid.org/0009-0003-7575-7497
Anifa D. Paluanova, https://orcid.org/0009-0007-7283-5604

REFERENCES

[1] A. Herz, D. Wang, R. Müller, and P. Schaaf, "Formation of supersaturated Au–Ni nanoparticles via dewetting of an Au/Ni bilayer," Mater. Lett. **102-103**, 22–25 (2013). https://doi.org/10.1016/j.matlet.2013.03.096
[2] M. Sang, K. Kang, Y. Zhang, H. Zhang, K. Kim, M. Cho, J. Shin, J.H. Hong, T. Kim, Sh.K. Lee, W.H. Yeo, J.W. Lee, T. Lee, B. Xu, and K.J. Yu, "Ultrahigh Sensitive Au-Doped Silicon Nanomembrane Based Wearable Sensor Arrays for Continuous Skin Temperature Monitoring with High Precision," Adv. Mater. **34**(4), 2105865 (2022). https://doi.org/10.1002/adma.202105865
[3] G.R. Moghal, "Chemical-bond model for gold surface states in gold doped silicon/silicon dioxide structures," Int. J. Electronics, **53**(3), 271-279 (1982). https://doi.org/10.1080/00207218208901509
[4] W.R. Thurber, D.C. Lewis, and W.M. Buillis, "Resistivity and carrier life time in gold - doped silicon," Electronic Technology Division Institute for Applied Technology National Bureau of Standards Washington, D.C. 20234, (1973). https://nvlpubs.nist.gov/nistpubs/Legacy/IR/nbsir73-128.pdf
[5] S.O. Konorov, H.G. Schulze, M.W. Blades, and R.F.B. Turner, "Silicon−Gold−Silica Lamellar Structures for Sample Substrates That Provide an Internal Standard for Raman Microspectroscopy," Anal. Chem. **86**(19), 9399–9404 (2014). https://doi.org/10.1021/ac501922a
[6] M. Aono, M. Takahashi, H. Takiguchi, Y. Okamoto, N. Kitazawa, and Y. Watanabe, "Thermal annealing of a-Si/Au superlattice thin films," Journal of Non-Crystalline Solids, **358**(17), 2150-2153 (2014). https://doi.org/10.1016/j.jnoncrysol.2011.12.088
[7] K. Fukami, M.L. Chourou, R. Miyagawa, A.M. Noval, T. Sakka, M. Manso-Silván, R.J. Martin-Palma, and Y.H. Ogata, "Gold Nanostructures for Surface-Enhanced Raman Spectroscopy, Prepared by Electrodeposition in Porous Silicon," Materials, **4**, 791-800 (2011). https://doi:10.3390/ma4040791
[8] D. Beeman, R. Tsu, and M.F. Thorpe, "Structural information from the Raman spectrum of amorphous silicon," Phys. Rev. B, **32**, 874 (1985). https://doi.org/10.1103/PhysRevB.32.874
[9] P. Danesh, B. Pantchev, K. Antonova, E. Liarokapis, B. Schmidt, D. Grambole, and J. Baran, "Hydrogen bonding and structural order in hydrogenated amorphous silicon prepared with hydrogen-diluted silane," J. Phys. D, **37**, 249 (2004). https://doi.org/10.1088/0022-3727/37/2/013
[10] R. Tsu, J.G. Hernandez, and F.H. Pollak, "Determination of energy barrier for structural relaxation in a-Si and a-Ge by Raman scattering," J. NonCryst. Solids, **66**, 109 (1984). https://doi.org/10.1016/0022-3093(84)90307-7
[11] Z.Q. Cheng, H.Q. Shi, P. Yu, and Z.M. Liu, 'Surface - enhanced Raman scattering effect of silver nanoparticles array," Acta Phys. Sin. **67**(19), 197302 (2018). https://doi.org/10.7498/aps.67.20180650
[12] F. Huisken, H. Hofmeister, B. Kohn, M.A. Laguna, and V. Paillard, "Laser production and deposition of light-emitting silicon nanoparticles," Appl. Surf. Sci. **154–155**, 305 (2000). https://doi.org/10.1016/s0169-4332(99)00476-6
[13] V. Vinciguerra, G. Franzo, F. Priolo, F. Iacona, and C. Spinella, "Quantum confinement and recombination dynamics in silicon nanocrystals embedded in Si/SiO_2 superlattices," J. Appl. Phys. **87**, 8165 (2000). https://doi.org/10.1063/1.373513
[14] Zh. Ma, X. Liao, J. He, W. Cheng, G. Yue, Y. Wang, and G. Kong, "Annealing behaviors of photoluminescence from SiO_x:H," J. Appl. Phys. **83**, 7934 (1998). https://doi.org/10.1063/1.367973
[15] S. Zhang, W. Zhang, and J. Yuan, "The preparation of photoluminescent Si nanocrystal–SiO_x films by reactive evaporation," Thin Solid Films, **326**, 92 (1998). https://doi.org/10.1016/S0040-6090(98)00532-X
[16] J. Zi, H. Buscher, C. Falter, W. Ludwig, K. Zhang, and X. Xie, "Raman shifts in Si nanocrystals," Appl. Phys. Lett. **69**, 200 (1996). https://doi.org/10.1063/1.117371
[17] Kh.S. Daliev, Z.E. Bahronkulov, and J.J. Hamdamov, "Investigation of the Magnetic Properties of Silicon Doped with Rare-Earth Elements," East Eur. J. Phys. **(4),** 167 (2023). https://doi.org/10.26565/2312-4334-2023-4-18
[18] Kh.S. Daliev, Sh.B. Utamuradova, Z.E. Bahronkulov, A.Kh. Khaitbaev, and J.J. Hamdamov, "Structure Determination and Defect Analysis n-Si<Lu>, p-Si<Lu> Raman Spectrometer Methods," East Eur. J. Phys. (4), 193 (2023). https://doi.org/10.26565/2312-4334-2023-4-23
[19] K.J. Kingma, and R.J. Hemley, "Raman spectroscopic study of microcrystalline silica," American Mineralogist, **79**(3-4), 269-273 (1994). https://pubs.geoscienceworld.org/msa/ammin/article-pdf/79/3-4/269/4209223/am79_269.pdf
[20] Sh.B. Utamuradova, H.J. Matchonov, Zh.J. Khamdamov, and H.Yu. Utemuratova, "X-ray diffraction study of the phase state of silicon single crystals doped with manganese," New Materials, Connections Oath Applications, **7**(2), 93-99 (2023). http://jomardpublishing.com/UploadFiles/Files/journals/NMCA/v7n2/Utamuradova_et_al.pdf
[21] Kh.S. Daliev, Sh.B. Utamuradova, J.J. Khamdamov, and M.B. Bekmuratov, "Structural Properties of Silicon Doped Rare Earth Elements Ytterbium," East Eur. J. Phys. (1), 375-379 (2024). https://doi.org/10.26565/2312-4334-2024-1-37

ВПЛИВ ЗОЛОТА НА СТРУКТУРНІ ДЕФЕКТИ КРЕМНІЮ

Шаріфа Б. Утамурадова[a], Шахрух Х. Далієв[a], Алішер Хайтбаєв[a], Джонібек Дж. Хамдамов[a], Улугбек М. Юлдошев[a], Аніфа Д. Палуанова[b]

[a]Інститут фізики напівпровідників та мікроелектроніки Національного університету Узбекистану, Ташкент, вул. Янгі Алмазара, 20, Узбекистан

[b]Нукуський державний педагогічний інститут імені Аджиніяза, Нукус, Узбекистан

У цьому дослідженні було проведено комплексне дослідження впливу легування кремнію золотом на оптичні властивості та морфологію шарів кремнію. Для цього використовували методи раманівської спектроскопії, інфрачервоної спектроскопії з перетворенням Фур'є (FTIR) та скануючої електронної мікроскопії (SEM). Результати дослідження показали, що перехід від вихідного кремнію до легованого золотом кремнію призводить до значних змін оптичних властивостей і морфології шарів. Спектри КРС показали характерні піки в областях 144, 304, 402, 464, 522, 948 і 973 см–1, пов'язані з порушенням дальнього порядку кристалічної решітки та взаємодією золота з кремнієм. Інтенсивність і положення піків у спектрах дозволили зробити висновки про структурні зміни, включаючи зниження кристалічності та утворення аморфних і нанокристалічних структур у зразках після обробки при 1373 К. Нові піки в спектрах КРС, пов'язані з Au Розтягування -Au і утворення нових зв'язків Si - Au, підтверджують процеси в шарах кремнію при сплаві золотом. Дослідження СЕМ дали інформацію про структуру, хімічний склад і розташування зразків n-Si-Au і p-Si-Au. Експериментально встановлено сферичне розташування атомів золота на поверхні монокристалічного кремнію, що свідчить про дифузію золота та утворення силікату золота, який вносить позитивний заряд на поверхню розділу. Морфологічні зміни включали збільшення кількості агломератів з розміром нанокристалів менше 7–9 нм та збільшення прозорості шару. Ці результати вказують на можливість покращення фоточутливості гетероструктур із композитним шаром Si–Au за рахунок квантово-розмірного та плазмонного ефектів включень, що містять наночастинки кремнію та золота.

Ключові слова: *кремній; золото; раманівська спектроскопія; інфрачервона спектроскопія; дифузія; скануюча електронна мікроскопія; термічна обробка; температура; компаунд*